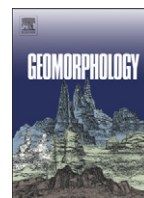




Contents lists available at SciVerse ScienceDirect

## Geomorphology

journal homepage: [www.elsevier.com/locate/geomorph](http://www.elsevier.com/locate/geomorph)

## Regolith transport quantified by braking block, McMurdo Dry Valleys, Antarctica

Jaakko Putkonen <sup>a,\*</sup>, Daniel J. Morgan <sup>b</sup>, Greg Balco <sup>c</sup><sup>a</sup> Department of Geology and Geological Engineering, MS 8358, University of North Dakota, Grand Forks, ND 58202, USA<sup>b</sup> Department of Earth and Environmental Sciences, Vanderbilt University, Nashville, TN 37240, USA<sup>c</sup> Berkeley Geochronology Center, 2455 Ridge Road, Berkeley, CA 94709, USA

## ARTICLE INFO

## Article history:

Received 18 November 2010

Accepted 7 December 2011

Available online xxxxx

## Keywords:

Regolith transport

Dry Valleys

Antarctica

Braking block

Landscape evolution

Topographic diffusivity

## ABSTRACT

The McMurdo Dry Valleys of Antarctica are today a hyper-arid, polar desert. Prior work has identified several in situ volcanic ashes (6–11 Myr old) resting on the surface regolith that suggests the persistent stability of the regolith surfaces and climate. However, our field observations of characteristic regolith bulges above and cavities below boulders that are lodged in the hillslope (braking blocks) contradict the apparent preservation of the regolith surfaces. To quantify the regolith mobility we modeled the downslope regolith transport around large boulders in the Dry Valleys using a finite difference regolith-transport model. To guide our modeling effort, we surveyed the detailed topography around one large boulder in the field. Model results fit the observed topography well and allow for the calculation of the minimum volume of regolith per unit width of slope that was mobilized ( $> 4 \text{ m}^3/1 \text{ m width}$ ). To assess the general applicability of the braking block analysis on random boulders on hillslope we surveyed the topographic characteristics adjacent to 997 boulders on 10 separate hillslopes. The bulge-cavity development appears to be sensitive to: 1) the adjacent obstructions that restrict the free movement of the regolith around the given boulder, and 2) the inherent surface roughness. Even though, theoretically boulders of all sizes should have a cavity-bulge pair surrounding them, the signal to noise ratio prevented us from extracting such measurements reliably on boulders whose diameter was smaller than about 1 m, on boulders that sat on bedrock covered by a thin veneer of regolith, and on boulders that were part of an actively aggrading talus. The limiting minimum topographic diffusivity was found to be  $10^{-6} \text{ m}^2/\text{yr}$ . Over time periods of millions of years this is enough to rework the surfaces and highlights the intriguing contradiction between the preserved ashes and the observed regolith transport.

© 2011 Elsevier B.V. All rights reserved.

## 1. Introduction

The McMurdo Dry Valleys of Antarctica (hereafter Dry Valleys) are the largest ice-free area in the continent and are located about 80 miles west of McMurdo research station, the main U.S Antarctic Program (USAP) logistical hub on Ross Island (Fig. 1). The mean annual air temperature in the field area is  $-24^\circ\text{C}$  (Putkonen et al., 2003). Precipitation occurs only as falling snow or as snow drifting from the ice sheet. The typically small amount of snow that precipitates annually sublimates directly into the air or melts on solar-heated rocks, then evaporates. Small amounts of water wet the regolith surface infrequently (Hagedorn et al., 2007). In the alpine valleys ( $> 1000 \text{ masl}$ ) running water is seldom seen, although we have observed small active rivulets, and small, dry, recently eroded channels and related small sediment fans.

Prior research has revealed a number of  $^{40}\text{Ar}/^{39}\text{Ar}$  dated volcanic ashes that are preserved in their primary depositional locations covering regolith in the Dry Valleys (Marchant et al., 1993a, b, 1996;

Sugden et al., 1995; Marchant and Denton, 1996; Lewis et al., 2006, 2007). The oldest of these ashes ranges between 6.4 and 11.3 Myr old, suggesting almost perfect preservation of regolith surfaces. Here we call regolith "... the loose, incoherent mantle of rock fragments, soil, glacial drift, blown sand, etc. that rests upon solid bedrock" (Whitten and Brooks, 1987).

This preservation of ashes on regolith surfaces and the existence of millions of years old ash avalanche (mixed ash and regolith) deposits on relatively steep  $28^\circ$  slopes imply unprecedented stability of regolith surfaces. However, several lines of evidence suggests general mobility and disturbance of the regolith in the same field area: the modeling of resurfacing time of patterned ground (Sletten et al., 2003), direct measurements of current sediment transport (Putkonen et al., 2008a), fluvial erosion by meltwater channels (Atkins and Dickinson, 2007), and re-interpretation (Ng et al., 2005) of a published cosmogenic depth profile (Schäfer et al., 2000) near one Miocene age ash deposit in Beacon Valley (Sugden et al., 1995). Moreover, cosmogenic isotope profiles in Dry Valleys have revealed a persistent surface degradation on average of  $1.2 \text{ m/Ma}$  (Putkonen et al., 2008b; Morgan et al., 2010a, b). Therefore ample motivation exists to better understand the rates and geomorphological processes that shape the Dry Valleys landscape.

\* Corresponding author. Tel.: +1 701 777 3213; fax: +1 701 777 4449.  
E-mail address: [jaakko.putkonen@engr.und.edu](mailto:jaakko.putkonen@engr.und.edu) (J. Putkonen).

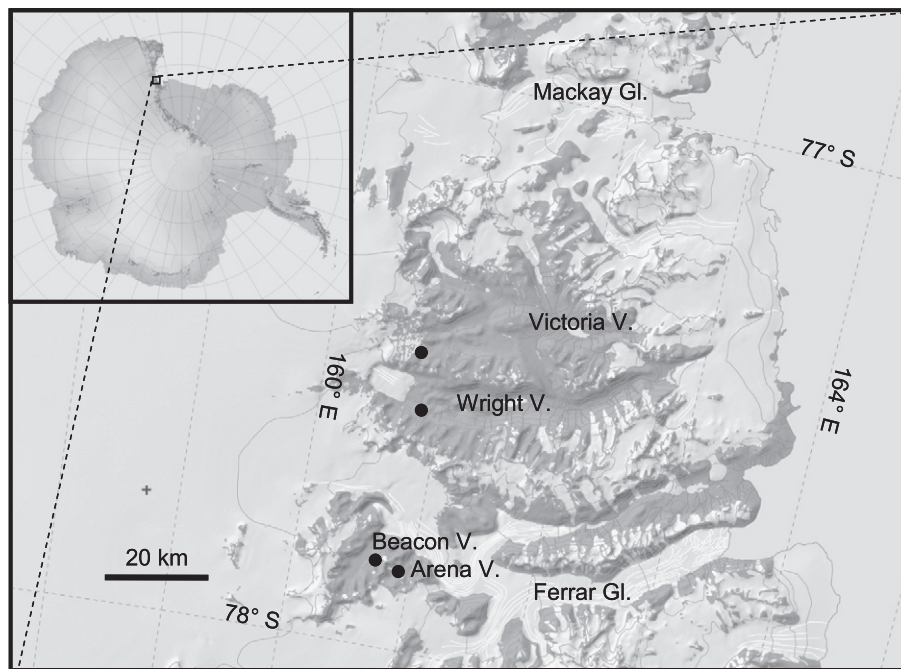


**Fig. 1.** Map of the McMurdo Dry Valleys region with an inset map of Antarctica. Snow and ice are white and ice-free areas are gray. Braking blocks were measured in the areas represented by the black dots.

Our recent field work in the Dry Valleys revealed a large number of boulders on hillslopes with a characteristic bulge of regolith piled against the uphill side of the boulder and a corresponding cavity on the downhill side of the boulder. These features (Fig. 2A, B) have been previously reported in the Arctic and have been called braking blocks by several authors (Höllerman, 1964; Graf, 1976; Washburn, 1979; Åkerman, 1980). We agree with those authors' conceptual model: the regolith is moving past the boulder down the hill while the boulder is stationary or travels at a relatively slower speed than the regolith surrounding it. Although typically found and described in the Arctic, these braking blocks can be found in other climates and parts of the world as well (Fig. 2C). We suggest that in environments where minimal or no regolith transport is expected, these braking blocks may be used as clear indicators of regolith mobility.

In the Dry Valleys we know that all the regolith transport is limited to the very surface of the soil (~1 cm) as the published cosmogenic isotope profiles attest of no mixing of the regolith below about 1 cm from the surface (Putkonen et al., 2008b; Morgan et al., 2010a, b).

In the following sections we use our field observations of braking blocks with a numerical model in an attempt to constrain the minimum amount of regolith that is transported downhill on a hillslope. We seek to establish if the regolith-transport rate is consistent with the apparent extreme preservation of the surfaces and deposits that are found on relatively steep slopes. As a byproduct of this quest, we will determine the corresponding limiting minimum topographic diffusivity for this environment.

## 2. Model and methods

Based on our own field experience in Antarctica, the braking blocks are ubiquitous and the simplest interpretation of their presence suggests mobility of the regolith. We surveyed one large braking block and its surroundings in the field to compare the characteristic topography with the modeled topography of a regolith transported past a stationary obstacle.

The detailed topography around one representative large braking block was surveyed just east of the Koenig Valley mouth at an altitude of about 1500 masl in western Wright Valley (McMurdo Dry Valleys,

Antarctica). The boulder is located in the undifferentiated colluvium whose minimum age in the Asgard Range has been determined to be 12 Myr (Marchant et al., 1993a). The regolith topography and boulder dimensions were determined by manual surveying of profiles down the steepest slope and across slope. Typical horizontal node spacing along the survey lines was 0.25 m (uncertainty  $\pm 0.025$  m). The relative surface elevations were rounded to closest 0.005 m (uncertainty  $\pm 0.01$  m).

In addition to recording a detailed topography of one large representative boulder, we also surveyed 10 transects on hillslopes in several valleys to cover a selection of slope aspects, slope angles, and types of slopes (scree under a vertical cliff, thinly mantled bedrock slope, and thick regolith away from cliff faces). On these transects we followed a path of steepest descent down the representative segment of the slope. Every boulder larger than 0.5 m in diameter within a 2.25 m wide swath down the slope was analyzed for the following attributes: cavity/no cavity, bulge/no bulge, maximum cavity depth below general slope, maximum bulge height above general slope, boulder width (cross slope direction), boulder length (down slope direction), boulder height above general slope, and local slope angle. These transects were about 500 m long. A clinometer, handheld GPS, and a tape measure were used to determine the general slope along the transect, position of the boulder, and the dimensions of the boulder, bulge, and cavity. The measurement accuracies are generally within a few cm for dimensions and about  $1^\circ$  for the slope. However, the generally bouldery surfaces forced us to decide whether to place the tape measure on top of a surface rock or between rocks when measuring for example the cavity depth. This issue will be visited again in the discussion section. Table 1 shows the coordinates for the starting point (upper end) and the type of slope for each transect.

### 2.1. Regolith-transport processes

It is not known what specific geomorphic processes move the regolith, mineral particles and pebbles, down slopes in the Dry Valleys over periods of millions of years. The field area is known today for strong winds which are well represented in the characteristic wind statistics that we recorded at the Beacon Valley: mean daily wind

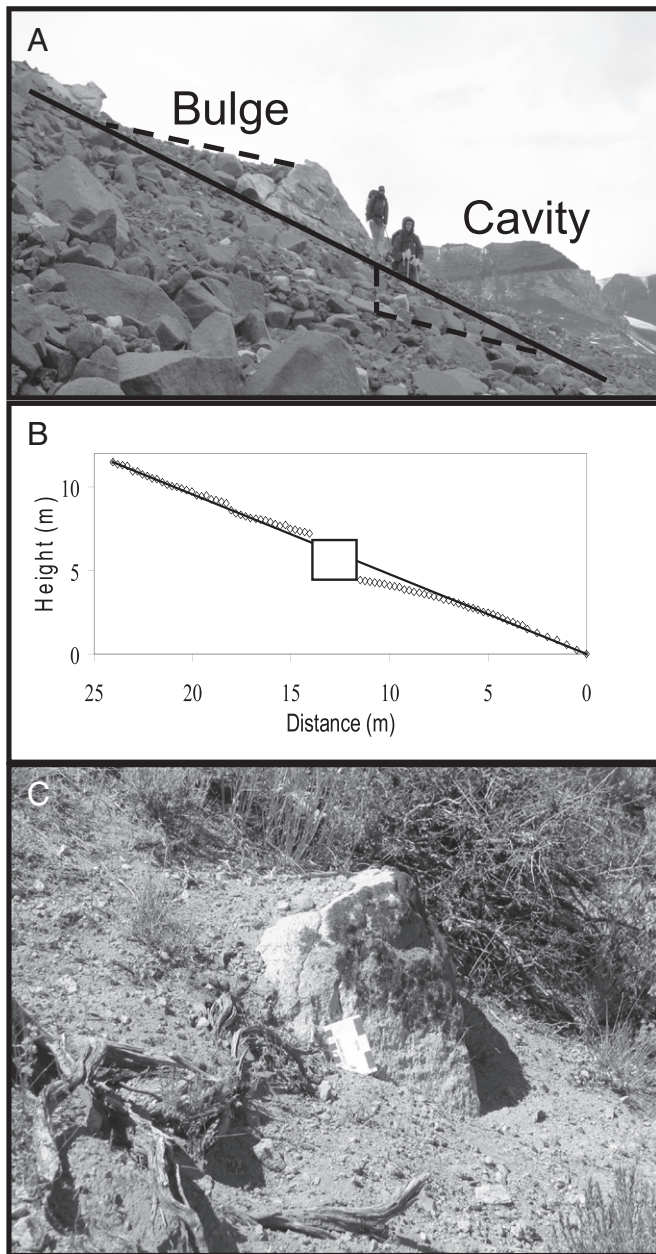


**Fig. 2.** A) A braking block with the characteristic convergence of material above the boulder, creating the bulge, and the corresponding divergence of material below the boulder, creating a cavity. B) The surveyed topographic profile downslope through the middle of the boulder shown in (A). The diamonds are the surveyed heights at 0.25 m horizontal spacing. The black line represents the average slope for area surrounding the braking block. C) A braking block on a moraine near Mono Lake, CA. In all panels the regolith is moving downhill from left to right.

speed was  $4.2 \text{ m s}^{-1}$  (all data for the period 1/1/2001–12/31/2003), mean of maximum daily 15 min wind speeds is  $7.6 \text{ m s}^{-1}$ , and the max 15 min wind speed is  $22 \text{ m s}^{-1}$ . We speculate that typically strong winds in the area may toss pebbles and sand in random directions, but due to the gravity the particles are most likely to travel to the downslope direction which results in the net mass transport down the steepest local slope. Wind erosion may also destabilize larger particles by removing the smaller particles that support them, after which the large particles would roll down the steepest local slope. This type of regolith movement would be restricted to the thin surface layer ( $\sim 1 \text{ cm}$ ) leaving all partially buried rocks firmly anchored in the regolith. This conceptual model is supported by a cosmogenic

isotope profile from a hillslope in Arena Valley that shows no soil mixing in the regolith below the surface for approximately the last 2 Myr and steady degradation (loss of mineral matter) at the surface (Putkonen et al., 2008b). Additional support is provided by repeat photography in the same field area that has shown individual pebbles moving predominantly downhill over the course of one year and accumulating in the regolith traps that were set up (Putkonen et al., 2008a).

Although reported in another part of the Antarctic continent, frost heave seems unlikely to move the regolith at this site as we know that the movement is restricted to the soil surface. Daily frost heave cycles of up to a maximum of 3.4 mm were recorded (Matsuoka and Moriwaki, 1992) when the regolith moisture content exceeded 5%. The heave was suggested to have contributed to the downslope movement of surficial regolith at a rate of up to 0.015 m/yr.

The regolith moisture content at our field site has not been measured. However, the age of the undifferentiated colluvium where the surveyed braking block is situated is more than 12 Myr (Marchant et al., 1993a). Bockheim (2002) found that the dry permafrost (as opposed to ice cemented) is pervasive on drifts older than 1 Myr. Campbell et al. (1998) report average moisture contents ranging from 1.5% in the Beacon Heights to 3% in the Coombs Hills and Convoy Range, which are located in or adjacent to the Dry Valleys, and are comparable in topography and climate to our site. For these reasons we suggest that frost heave is unlikely to be active at our field site today, but we cannot rule it out from having occurred in the past.

## 2.2. Numerical regolith-transport model

Next we will mathematically formulate the model that relates the rate of regolith movement downhill to the local slope angle. In the model it is assumed that the regolith is preferentially transferred downslope due to unspecified geological processes over the period of the braking block formation, such as wind, freeze/thaw cycles, and running water.

The general regolith-transport model that mathematically describes the evolution of a was originally formulated by Culling (1960, 1963, 1965) and since then has been widely used (e.g. Carson and Kirkby, 1972; Nash, 1980; Hanks et al., 1984; Hallet and Putkonen, 1994; Fernandes and Dietrich, 1997; Heimsath et al., 1997; Roering et al., 2001; Putkonen and Swanson, 2003; Putkonen and O'Neal, 2006; Putkonen et al., 2008c). The general formulation can be applied to the regolith that surrounds a braking block by inserting an obstruction to the regolith flow into the model domain. The boundary between the obstruction and the regolith is assumed to have the same properties as any boundary between two adjacent regolith model cells. The hillslope model has an initially smooth and straight profile with one protruding boulder located in the center. This initial condition seems reasonable in view of the typical rectilinear slopes observed in the field area today (Selby, 1971). The model domain boundaries are defined adiabatic which mimics the effect of an infinitely long hillslope so that the upper and the lower boundaries do not affect the results. This is a reasonable convention given the typical length of the slopes of 100 s of meters and the assumed slow regolith-transport rate. The mathematical formulation given below generally follows the derivation that was clearly presented by Hanks et al. (1984) and Fernandes and Dietrich (1997) both based on original ideas by Culling (1960).

Typically, the regolith transport on a hillslope is viewed as resulting from progressive and intermittent downslope motion of the regolith. Both components of the total regolith flux ( $q_x$  and  $q_y$  [ $\text{kg/m yr}$ ]) in two orthogonal horizontal directions  $x$ , and  $y$  are proportional to the transport coefficient ( $k$ ) expressed in ( $\text{kg/m yr}$ ) and the corresponding slope inclination,  $\partial z/\partial x$  or  $\partial z/\partial y$ , where  $z$  is vertical dimension (m) and  $x$  and  $y$  are horizontal dimensions (m). The simplest

**Table 1**  
Survey details of the ten transects surveyed for the occurrence of braking blocks. The starting locations of the transects are given and from there the transect follows a path of steepest descent down the slope for approximately 500 m. Cavity statistics are reported for only those boulders that had measurable cavities.

#	Site	Lat (S) degrees	Long degrees	Mean cavity depth (cm)	Max cavity depth (cm)	Standard deviation of cavity depth (cm)	Mean boulder width (cm)	Standard deviation of boulder width (cm)	Mean boulder length (cm)	Standard deviation of boulder length (cm)	Missing data
1	Arena Valley	77.87282	160.93338	14.6	30	7.6	106.8	52.3	50.1	31.8	Yes
2	Arena Valley	77.85567	161.01373	5.3	10	4.2	65	5	35	7.1	Yes
3	Arena Valley	77.86555	160.8157	7.9	21	3.7	85.5	31.2	60.4	37.4	No
4	Arena Valley	77.8288	160.9733	13.4	23	3.7	84.4	34	59.1	17.9	No
5	Arena Valley	77.84312	160.99818	7.7	11	1.9	78.7	24.9	60.6	27.4	No
6	Beacon Valley	77.83933	160.72957	10.1	16	3.1	68.4	20.1	56.7	26.3	No
7	Wright Valley	77.57615	160.8138	8.8	21	2.8	67.1	18.7	54.8	20.3	No
8	Western Olympus Range	77.49048	160.97182	32.7	41	7.2	171.7	75.9	98.3	20.2	No
9	Western Olympus Range	77.46052	160.829	6.9	10	1.7	95.6	69.7	62.8	33.2	No
10	Western Olympus Range	77.471	160.81078	9.7	20	4.2	76.1	30.9	54.5	24.9	No

relation expressing the general increase in regolith flux with slope steepness is:

$$q_x = -k \frac{\partial z}{\partial x} \quad (1)$$

and

$$q_y = -k \frac{\partial z}{\partial y} \quad (2)$$

where  $q_x$  is the regolith flux in x-direction and  $q_y$  is the regolith flux to y-direction,  $k$  is assumed to be constant through space and time. The transport Eqs. (1) and (2) relating regolith flux to local slope, together with the expression for the conservation of mass lead to an expression relating the rate of change of the local surface elevation,  $\partial z / \partial t$ , to the divergence of local mass flux:

$$\frac{\partial z}{\partial t} = \frac{1}{\rho_s} \left( -\frac{\partial q_x}{\partial x} - \frac{\partial q_y}{\partial y} \right) \quad (3)$$

where  $\rho_s$  is regolith bulk density ( $\text{kg/m}^3$ ), and  $t$  is time (yr). This relation is applicable for any regolith-transport process, but excludes such complications as solute transport, weathering of the matrix, aeolian deposition or deflation, and time-dependent changes in regolith density.

Combining Eqs. (2) with 3 leads to a diffusion equation for topographic evolution in two dimensions:

$$\frac{\partial z}{\partial t} = \kappa \left( \frac{\partial^2 z}{\partial x^2} \right) + \kappa \left( \frac{\partial^2 z}{\partial y^2} \right) \quad (4)$$

where  $\kappa$  ( $\text{m}^2/\text{yr}$ ) is  $k/\rho_s$ . With proper boundary conditions this equation can readily be solved numerically with a finite difference approximation.

### 2.3. Conceptual description of the topographic evolution

This section describes qualitatively the evolution of the regolith topography adjacent to a braking block from an initially straight slope to fully developed bulge/cavity topography.

The hillslope in the model has an initially straight profile at an angle of  $24^\circ$  (the observed general slope angle around the surveyed large braking block) that is interrupted only by a half-exposed

spherical boulder in the middle of the slope whose radius ( $r$ ) matches the observed braking block in the field ( $2r = 4.4$  m). This initial model state resembles a step change or an instantaneous disturbance in the sense that the regolith that is being transported downhill adjacent to the boulder is not in a steady-state configuration with the boulder. This initial state can be thought to represent the hillslope soon after it was exposed by a receding ice sheet.

The regolith is transported down the steepest local slope at a rate that is proportional to the local slope angle. This continuous flux of regolith down the hill is obstructed by the stationary boulder in the middle of the slope which forces the regolith to move either around or onto the boulder. Initially, the local slope immediately above the boulder becomes gentler, which facilitates the net deposition of regolith in that domain. However, as regolith ramps against and above the boulder (creating the bulge), the local lateral slopes on both sides of the boulder slowly increase in steepness. These side slopes will eventually grow steeper than the original slope to effectively shed all the regolith that is redirected sideways from the bulge directly above the boulder.

The cavity immediately down slope of the boulder reflects the initial discrepancy between the unimpeded regolith flux downhill out of the cavity area and the lack of incoming regolith flux into the cavity due to the obstruction by the boulder. As the cavity deepens the side slopes will become steeper and start shedding regolith more efficiently into the cavity. This will eventually lead into a dynamic balance where the regolith flux from the steeper side slopes will exactly match the outflow of regolith from the cavity.

When the final steady-state topography surrounding the boulder is compared to the initial straight and rectilinear regolith surface the following differences are noted: 1) upslope of the boulder a ramp has formed whose top surface is almost flat, however, the side slopes of the ramp are steep, 2) down slope of the boulder an almost flat floored cavity has been formed, and 3) the regolith surface on both sides of the boulder (looking downhill) has become steeper than they were initially. This is because the ramp above the boulder has advanced partially over the boulder and the cavity below the boulder has partially undercut the boulder. These steeper than initial side slopes allow the transportation of an increased amount of regolith per unit width of the slope that is now skirting the boulder.

### 2.4. Model time and topographic diffusivity

For short slopes,  $\kappa$  typically ranges between  $10^{-1}$  and  $10^{-4} \text{ m}^2 \text{ yr}^{-1}$  (Hanks et al., 1984; Fernandes and Dietrich, 1997;

Hanks, 2000; Oehm and Hallet, 2005) and between  $10^{-4}$  and  $10^{-5} \text{ m}^2 \text{ yr}^{-1}$  today in the Dry Valleys (Putkonen et al., 2008a). The model yields topographic evolution through time, including the formation of the bulge above and cavity below the stationary boulder. The resulting surface topography is uniquely dependent of the combination of elapsed time and topographic diffusivity until the model reaches steady state.

A finite difference approximation of Eqs. (4) is used to model the time-dependent evolution of the regolith topography around a partially exposed boulder. In this scheme it is not possible to solve simultaneously for the two unknowns: elapsed model time ( $t_{\text{tot}}$ ) and the topographic diffusivity ( $\kappa$ ). However, by describing the initial (assumed) and final surface topographies (measured in the field) it is possible to find a unique combination (product) of the time and topographic diffusivity that results in the best fit between the observed and modeled topographies. We stress that the absolute value of neither parameter can be obtained, but their product can be.

For example if the absolute value of the topographic diffusivity in the model is decreased the regolith topography will evolve slower. However, to reach the same final topography the total elapsed time needs to be increased, which will allow the topography to evolve longer and the unique product of  $\kappa t_{\text{tot}}$  is maintained. If the product of  $\kappa t_{\text{tot}}$  is the same, but with a high topographic diffusivity and a short elapsed model time, the same final topography is achieved. This is to say that the resulting topography is independent of the chosen parameter values as long as the unique product remains constant.

### 2.5. Definition of the steady state

The diffusive response to an instantaneous disturbance or a step change is typically asymptotic in nature. The new equilibrium is approached at a decreasing rate of change. It therefore becomes necessary to unequivocally define a point where the model has reached an adequate approximation of the steady state. Ahnert (1987) and Fernandes and Dietrich (1997) suggested that when the model surface has reached 90% of the maximum possible change in surface elevation it would be an adequate approximation of the steady-state topography. In our modeling we track the depth of the cavity and the height of the bulge, which are the features that experience the largest elevation change. The maximum change in height or depth was defined as the maximum elevation change that the bulge or cavity reached when the model was allowed to run for millions of years. When both of these features have reached 90% of their maximum height or depth we are satisfied that the model has reached an adequate approximation of the steady state. Later in the paper we will discuss the sensitivity of the results to this choice.

### 2.6. Total regolith transport past the boulder

To calculate the total regolith transport,  $Q_{\text{tot}}$  ( $\text{m}^2$ , or rather cubic meters per 1 m width of the slope) Eqs. (5), we divide Eqs. (1) by regolith bulk density  $\rho_s$  ( $\text{kg}/\text{m}^3$ ) and multiply it by total elapsed time  $t_{\text{tot}}$  (yr).

$$Q_{\text{tot}} = t_{\text{tot}} q_n. \quad (5)$$

Combining Eq. (1) in general n-dimension with Eq. (5) results in:

$$Q_{\text{tot}} = t_{\text{tot}} \kappa \frac{\partial z}{\partial n}. \quad (6)$$

Thus, if we know the unique combination of  $\kappa t_{\text{tot}}$  required to form the bulge-cavity topography and the local slope ( $dz/dn$ ) then we can calculate the total regolith transport required to form the final steady-state topography.

### 2.7. Braking blocks on slope transects

To facilitate the analyses and presentation of the large number of cavity depths from the hillslope transects a dimensionless cavity size,  $L_c$ , is defined:

$$L_c = \frac{d_c}{W_b} \quad (7)$$

where  $W_b$  is boulder width (m),  $d_c$  is cavity depth (m).

## 3. Results

### 3.1. Steady-state profiles

The model tracks the absolute differences between three modeled and observed topographic profiles A–A', B–B', and C–C' (Fig. 3A, B, and C). The qualitatively close match between observed and modeled profiles suggests that the model captures the essence of the regolith transport. The least difference and therefore the best fit between modeled and observed surface elevations for all profiles are found at modeled steady state, which suggests that the observed topography has reached steady state. Therefore, it is possible that much more regolith has been transported past the braking block since it reached the steady state. Thus, we can only calculate the minimum regolith transport required to create this bulge and cavity pair. The analysis yields a conservative estimate of the regolith mobility.

It is important to note that the model contains no adjustable parameters that affect the steady-state topography. The only parameter that is allowed to vary in addition to the total time is the topographic diffusivity. The only effect of this parameter is to dictate how fast the regolith is transported across the landscape. It ultimately affects only the time that it takes to reach the steady state. Given this simple nature of the model we find it remarkable that the steady-state topography is qualitatively very close to the observed topography.

### 3.2. Total regolith transport past the boulder

For this braking block on a general slope ( $\partial z/\partial n$ ) of 0.44 (or  $24^\circ$ ), the unique product of  $\kappa t_{\text{tot}}$  that results the steady-state topography is  $10 \text{ m}^2$ . When these values are inserted into Eqs. (6) the result is the minimum total transport of  $4.4 \text{ m}^3$  of regolith per 1 m width of the slope over the entire lifespan of the hillslope.

### 3.3. Topographic diffusivity

The minimum limiting age for the undifferentiated colluvium where the boulder is embedded has been determined to be 12 Myr (Marchant et al., 1993a). A minimum estimate of the topographic diffusivity can be calculated if this known maximum limiting age ( $t_{\text{tot}}$ ) is inserted into the  $\kappa t_{\text{tot}} = 10 \text{ m}^2$ . This results in a minimum estimate for the topographic diffusivity of  $10^{-6} \text{ m}^2/\text{yr}$ . This limiting minimum value is one to two orders of magnitude smaller than any previously reported value for topographic diffusivity elsewhere on Earth or in the Dry Valleys (Hanks et al., 1984; Fernandes and Dietrich, 1997; Hanks, 2000; Oehm and Hallet, 2005; Putkonen et al., 2008a).

### 3.4. Braking blocks on slope transects

In the ten slope transects we counted a total of 997 boulders and found measurable cavity-bulge pairs on 190 of these boulders. An additional 265 boulders had a faint cavity and/or bulge that could not be accurately measured.

We found that although numerous on the slopes the boulders whose diameter were less than 1 m had in theory and practice cavities that were too small for us to measure them with high enough

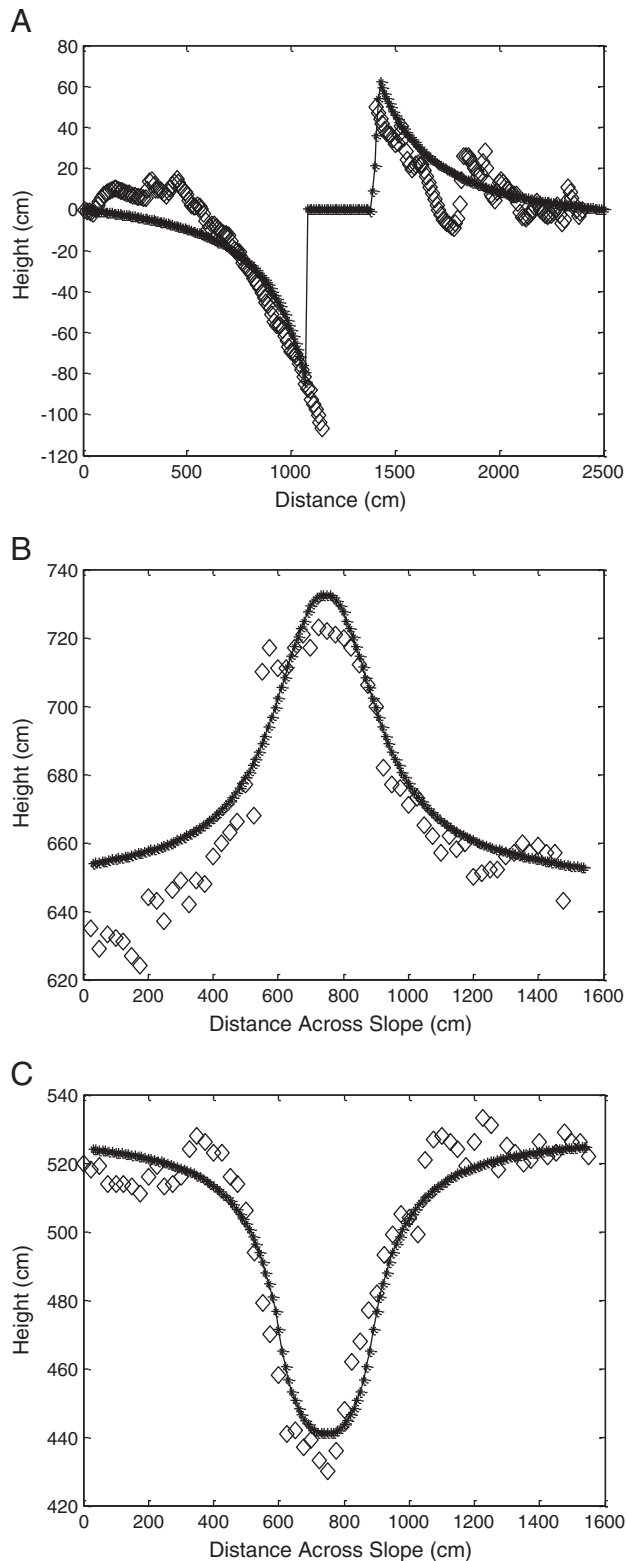


**Fig. 3.** All three figures compare the measured topographic profile to the modeled profile. The open diamonds are the points measured in the field and the asterisks connected by a line are the model results. A) The downslope survey through the middle of the boulder compared to the center line model results. The horizontal distance in the figure increases upslope. Both profiles show only the deviation from the general slope. B) Across-slope profile surveyed upslope of the boulder showing the bulge of the braking block. C) Across-slope profile surveyed downslope of the boulder showing the cavity of the braking block.

accuracy to produce meaningful results. Therefore the rest of the analysis is based on the boulders whose diameter is more than 1 m.

In Fig. 4 the relationship between the modeled dimensionless cavity size (Eqs. (7)) and the slope angle is shown (bold black line). For a given slope angle, the model predicts that the cavity depth scales with the boulder width, so that regardless of the boulder diameter the dimensionless cavity size is constant. The dimensionless cavity size predicted by the model increases linearly with the slope angle.

The expectation is that if all the measured cavities in the field are in steady state, and the measurements are accurate, then all the observations will plot on the modeled steady state line in Fig. 4. The data that plot below the model line have a cavity that is shallower than predicted for the measured slope angle and boulder width and vice versa.

To investigate the effect of measurement uncertainty on the calculated cavity sizes the data was separated into two groups based on the boulder width ( $W_b$ ):  $1\text{ m} \leq W_b < 2\text{ m}$ , and  $W_b \geq 2\text{ m}$ . Fig. 4 indicates that for large boulders ( $W_b \geq 1\text{ m}$ ) with larger cavities, we expect that the effects of the surface roughness will have a smaller relative error. The large boulders generally plot below the model line in Fig. 4, indicating that they have a shallower cavity depth than predicted by the model. Because larger braking blocks will take a longer period of time to fully form the bulge and cavity features (for a given topographic diffusivity), it is possible that steady-state has not yet been reached for these boulders and that the cavity, as measured, is not yet fully formed. It is also possible that as the cavity forms, it may undercut the boulder, allowing the boulder to move forward into the cavity, thus partially filling in the cavity.

#### 4. Discussion and conclusions

The preservation of millions of years old volcanic ashes and glacial moraines at or near the soil surface in the Dry Valleys of Antarctica has contributed to the impression of almost total stability of the landscape since deglaciation (e.g. Marchant et al., 1993a; Lewis et al., 2007). On the other hand braking blocks, are ubiquitous in the McMurdo Dry Valleys and suggest mobility of the regolith. A good fit

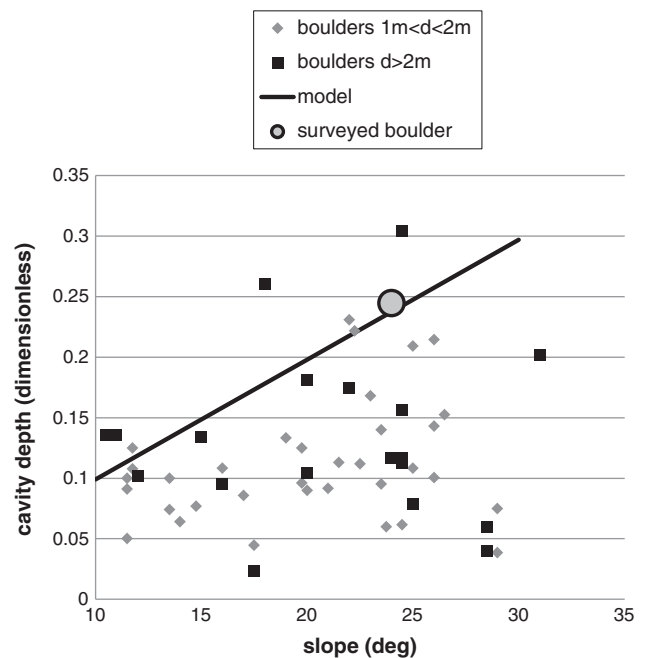


**Fig. 4.** The bold black line shows the modeled relation of the cavity size (dimensionless, see Eq. 7 for definition) to the slope angle in degrees. The bold black line divides the figure in two separate domains: the cavity depths below the line are deeper than predicted by the model at steady state and above the line they are shallower. The squares and diamonds denote dimensionless cavity depths on individual boulders that were surveyed in the field.

between modeled and measured braking block topography suggests that the model captures the essence of the regolith transport and shows that the topography surrounding the surveyed boulder has reached the steady state. Based on the transport model the minimum regolith transport past the boulder, is  $4.4 \text{ m}^3/1 \text{ m}$  width of the slope. The corresponding topographic diffusivity  $> 10^{-6} \text{ m}^2/\text{yr}$  is one to two orders of magnitude smaller than reported in Dry Valleys or elsewhere on Earth. We note that it is likely that the actual topographic diffusivity is larger than this because the bulge-cavity topography has reached steady state; the topography is therefore not sensitive to more regolith streaming by.

It is not obvious what the geomorphic process responsible for the regolith transport in this cold, arid environment might be assuming that the climate has remained unchanged for millions of years as suggested by Marchant et al. (1993b) and more recently by Lewis et al. (2007). Running water seems the least likely transport agent, because no rain is observed in this area today and only few signs of surface runoff have been witnessed, mainly from melting snow packs. The thermal contraction cracking of the ice-cemented regolith is active today and the resulting cracks can open and close totaling a movement of about  $10 \text{ mm/year}$  (Sletten et al., 2003). The resulting patterned ground is widespread in the area, and is found on some of the slopes where the braking blocks occur. However, it is not currently known if the annual contraction/expansion cycle of the dry regolith (as opposed to ice-cemented regolith) is enough to induce grain movement down the steepest local slope. Perhaps the most likely agent to move the regolith on the slopes is the wind as shown by Putkonen et al. (2008a).

To investigate the spatial variation in braking block properties a total of 997 boulders were measured on ten slope transects separated by 1–40 km. The smaller boulders (diameter  $< 1 \text{ m}$ ) on the gentle slopes (slope angle  $< 15^\circ$ ) revealed especially large scatter in dimensionless cavity depth as compared to the corresponding modeled steady-state dimensionless cavity depth (Fig. 4).

It is interesting to note that the cavity size on the one braking block that was chosen for the detailed survey falls very close to the modeled steady state for the given slope angle. It is assumed that the good fit between the model and observations is a result of the somewhat unusual conditions at that particular field site: 1) the measured boulder was unusually large (diameter =  $4.5 \text{ m}$ ) which ensures that small measurement errors are a relatively small fraction of the total dimensions, 2) the measured boulder is located several meters away from all adjacent large boulders, ensuring that the measured bulge and cavity have evolved without interference from adjacent boulders, and braking blocks, 3) the hillslope has a deep regolith cover, providing a steady supply of sediment. All these conditions were seldom met on the measured transects where every boulder with a diameter  $> 0.5 \text{ m}$  was measured regardless of its surroundings to ensure a representative and unbiased sample population.

We conclude that the braking blocks are sensitive indicators of regolith transport and are especially useful in an environment where little or no transport is expected. However, the development of the characteristic braking block topography in the terrain surrounding the boulder can be significantly affected by the surface roughness (frequency of surface boulders), and adjacent braking blocks. Therefore the surveys should be concentrated on slopes where relatively few large boulders impede the downhill transport of finer grains (Fig. 2C).

## Acknowledgements

This research was supported by the Office of Polar Programs, National Science Foundation grant #OPP-0338224 to Putkonen. We gratefully acknowledge the assistance in the field by J. Connolly, B. O'Donnell, N. Turpen, and K. Craig, and the logistical support by Raytheon Polar Services. The manuscript improved significantly by comments by J. Roering, R. S. Anderson, T. Hanks, and anonymous reviewers.

## Reference

- Ahnert, F., 1987. Approaches to dynamic equilibrium in theoretical simulations of slope development. *Earth Surface Processes and Landforms* 12, 3–15.
- Åkerman, J., 1980. Studies on periglacial geomorphology in west Spitsbergen. Meddelanden fran Lunds Universitets Geografiska Institution, 89. Lund, Sweden. 297 pp.
- Atkins, C.B., Dickinson, W.W., 2007. Landscape modification by meltwater channels at margins of cold-based glaciers, Dry Valleys, Antarctica. *Boreas* 36, 47–55.
- Bockheim, J.G., 2002. Landform and soil development in the McMurdo dry valleys, Antarctica; a regional synthesis. *Arctic, Antarctic, and Alpine Research* 34, 308–317.
- Campbell, I.B., Claridge, G.G.C., Campbell, D.I., Balks, M.R., 1998. The soil environment of the McMurdo Dry Valleys, Antarctica. In: Prisco, J. (Ed.), *Ecosystem Dynamics in a Polar Desert, the McMurdo Dry Valleys, Antarctica*. American Geophysical Union, Washington, D.C, p. 369.
- Carson, M.A., Kirkby, M.J., 1972. *Hillslope Form and Process*. Cambridge Geographical Studies, 3. Cambridge University Press, Cambridge, UK. 475 pp.
- Culling, W.E.H., 1960. Analytical theory of erosion. *Journal of Geology* 68, 336–344.
- Culling, W.E.H., 1963. Soil creep and the development of hillside slopes. *Journal of Geology* 71, 127–161.
- Culling, W.E.H., 1965. Theory of erosion on soil-covered slopes. *Journal of Geology* 73, 230–254.
- Fernandes, N.F., Dietrich, W.E., 1997. Hillslope evolution by diffusive processes: the timescale for equilibrium adjustments. *Water Resources Research* 33, 1307–1318.
- Graf, K.J., 1976. Zur Mechanik von Frostmusterungsprozessen in Bolivien und Ecuador. *Zeitschrift fur Geomorphologie* 20, 417–447.
- Hagedorn, B., Sletten, R., Hallet, B., 2007. Sublimation and ice condensation in hyper-arid soils: modeling results using field data from Victoria Valley, Antarctica. *Journal of Geophysical Research* 112. doi:10.1029/2006JF000580.
- Hallet, B., Putkonen, J., 1994. Surface dating of dynamic landforms; young boulders on aging moraines. *Science* 265, 937–940.
- Hanks, T.C., Bucknam, R.C., Lajoie, K.R., Wallace, R.E., 1984. Modification of wave-cut and faulting-controlled landforms. *Journal of Geophysical Research* 89, 5771–5790.
- Hanks, T.C., 2000. The age of scarplike landforms from diffusion-equation analysis. In: Noller, J.S., Sowers, J.M., Lettis, W.R. (Eds.), *Quaternary Geochronology Methods and Applications*, AGU Reference Shelf. American Geophysical Union, Washington, DC, p. 582.
- Heimsath, A.M., Dietrich, W.E., Nishiizumi, K., Finkel, R.C., 1997. The soil production function and landscape equilibrium. *Nature* 388, 358–361.
- Höllerman, P.W., 1964. Rezente verwitterung, abtragung und formenschatz in den Zentralalpen am Beispiel des oberen Studentental. *Zeitschrift fur Geomorphologie*, supplement 4, 1–257.
- Lewis, A.R., Marchant, D.R., Kowalewski, D.E., Baldwin, S.L., Webb, L.E., 2006. The age and origin of the Labyrinth, western Dry Valleys, Antarctica: evidence for extensive middle Miocene subglacial floods and freshwater discharge to the southern ocean. *Geology* 34, 513–516.
- Lewis, A.R., Marchant, D.R., Ashworth, A.C., Hemming, S.R., Machlus, M.L., 2007. Major middle Miocene global climate change: evidence from East Antarctica and the Transantarctic Mountains. *Geological Society of America Bulletin* 119, 1449–1461.
- Marchant, D.R., Denton, G.H., Sugden, D.E., Swisher, C.C.I., 1993a. Miocene glacial stratigraphy and landscape evolution of the western Asgard Range, Antarctica. *Geografiska Annaler. Series A: Physical Geography* 75, 303–330.
- Marchant, D.R., Denton, G.H., Swisher, C.C.I., 1993b. Miocene–Pliocene–Pleistocene glacial history of Arena Valley, Quartermain Mountains, Antarctica. *Geografiska Annaler. Series A: Physical Geography* 75, 269–302.
- Marchant, D.R., Denton, G.H., Swisher, C.C.I., Potter, N.J., 1996. Late Cenozoic Antarctic paleoclimate reconstructed from volcanic ashes in the dry valleys region of southern Victoria Land. *Geological Society of America Bulletin* 108, 181–194.
- Matsuoka, N., Moriwaki, K., 1992. Frost heave and creep in the Sør Rondane Mountains, Antarctica. *Arctic and Alpine Research* 24, 271–280.
- Morgan, D., Putkonen, J., Balco, G., Stone, J., 2010b. Quantifying regolith erosion rates with cosmogenic nuclides  $^{10}\text{Be}$  and  $^{26}\text{Al}$  in the McMurdo Dry Valleys, Antarctica. *Journal of Geophysical Research* 115 (F03037), 1–17.
- Morgan, D.J., Putkonen, J., Balco, G., Stone, J.O.H., 2010a. Degradation of glacial deposits quantified with cosmogenic nuclides, Quartermain Mountains, Antarctica. *Earth Surface Processes and Landforms* 36, 217–228.
- Nash, D.B., 1980. Forms of bluffs degraded for different lengths of time in Emmet County, Michigan, U.S.A. *Earth Surface Processes* 5, 331–345.
- Ng, F., Hallet, B., Sletten, R.S., Stone, J.O., 2005. Fast-growing till over ancient ice in Beacon Valley, Antarctica. *Geology* 33, 121–124.
- Oehm, B., Hallet, B., 2005. Rates of soil creep, worldwide: weak climatic controls and potential feedback. *Zeitschrift fur Geomorphologie* 49, 353–372.
- Putkonen, J., O'Neal, M.A., 2006. Degradation of unconsolidated Quaternary landforms in the western North America. *Geomorphology* 75, 408–419.
- Putkonen, J., Swanson, T., 2003. Accuracy of cosmogenic ages for moraines. *Quaternary Research* 59, 255–261.
- Putkonen, J., Sletten, R.S., Hallet, B., 2003. Atmosphere/ice energy exchange through thin debris cover in Beacon Valley, Antarctica. In: Phillips, M., Springman, S.M., Arenson, L.U. (Eds.), *Eighth international Conference on Permafrost*, Zurich, Switzerland, July 21–25, 2003. Swiss Federal Institute for Snow and Avalanche Research. Davos, Zurich, Switzerland, pp. 913–915.
- Putkonen, J., Rosales, M., Turpen, N., Morgan, D., Balco, G., Donaldson, M., 2008c. Regolith transport in the Dry Valleys of Antarctica. In: Cooper, A.K., Barrett, P.J., Stagg, H.,

- Storey, B., Stump, E., Wise, W. (Eds.), *Antarctica: A Keystone in Changing World*. Proceedings of the 10th International Symposium on Antarctic Earth Sciences. The National Academies Press, Santa Barbara, CA, USA. doi:10.3133/of2007-1047.srp103. 164 pp.
- Putkonen, J., Balco, G., Morgan, D., 2008a. Slow regolith degradation without creep determined by cosmogenic nuclide measurements in Arena Valley, Antarctica. *Quaternary Research* 69, 242–249.
- Putkonen, J., Connolly, J., Orloff, T., 2008b. Landscape evolution degrades the geologic signature of past glaciations. *Geomorphology* 97, 208–217.
- Roering, J.J., Kirchner, J.W., Sklar, L.S., Dietrich, W.E., 2001. Hillslope evolution by non-linear creep and landsliding: an experimental study. *Geology* 29, 143–146.
- Schäfer, J.M., Baur, H., Denton, G.H., Ivy-Ochs, S., Marchant, D.R., Schluchter, C., Wieler, R., 2000. The oldest ice on Earth in Beacon Valley, Antarctica: new evidence from surface exposure dating. *Earth and Planetary Science Letters* 179, 91–99.
- Selby, M.J., 1971. Slopes and their development in an ice-free, arid area of Antarctica. *Geografiska Annaler* 53A, 235–245.
- Sletten, R.S., Hallet, B., Fletcher, R.C., 2003. Resurfacing time of terrestrial surfaces by the formation and maturation of polygonal patterned ground. *Journal of Geophysical Research* 108 (E4), 8044.
- Sugden, D.E., Marchant, D.R., Potter, N.J., Souchez, R.A., Denton, G.H., Swisherand, C.C.I., Tison, J.L., 1995. Preservation of Miocene glacier ice in East Antarctica. *Nature* 376, 412–414.
- Washburn, A.L., 1979. *Geocryology: A Survey of Periglacial Processes and Environments*. Fletcher & Sons Ltd, Norwich, UK. 406 pp.
- Whitten, D.G.A., Brooks, J.R.V., 1987. *Dictionary of Geology*. Viking Penguin Inc, New York. 493pp.